SAR Image Formation as Wavelet Transform.

Jens Fischer, Thomas Molkenthin, German Aerospace Center, Oberpfaffenhofen, Germany
Madhu Chandra, Chemnitz University of Technology, Chemnitz, Germany
jens.fischer@dlr.de, thomas.molkenthin@dlr.de, madhu.chandra@infotech.tu-chemnitz.de

Abstract

In this paper, we derive the SAR raw data model by applying windowing, sampling and convolution to radar reflectivity. We define the SAR transform as the operation reversing the implicitly performed convolution by inverse convolution applied to SAR raw data. The SAR transform is then compared to both, Fourier and Wavelet transform. In either case, defocusing with a certain waveform is involved. We show that SAR and Fourier transform are two opposite special cases of the Wavelet transform in a slightly generalized sense. Due to the fact that the chirp signal which is generating SAR raw data, formally fulfills all requirements for being a wavelet, we conclude furthermore that there might exist faster SAR processing algorithms than those based on the Fourier transform and discuss the idea towards the goal of fast SAR processing, successively focusing in time domain.

1 Introduction

In recent years, the Wavelet transform has been shown to have numerous applications, especially, after techniques for the design of *fast* wavelet transforms have been discovered. Also in the field of Synthetic Aperture Radar the wavelet transform is used successfully in a great variety such as for SAR data compression, despeckling SAR images, for SAR image texture analysis and also for edge detection in SAR images as for finding coast lines. The wavelet chosen mainly depends on the intended application. However, the search for the most suitable wavelet in SAR raw data compression on one hand and great parallels between SAR processing and wavelet transforming on the other hand lead to the idea that SAR processing itself might be a wavelet transform. The idea is also investigated in [1] and the authors conclude that SAR imaging obviously appears as 'natural' arising wavelet application.

Indeed, the wavelet transform is closely related to SAR processing as can be seen by just looking at its definition for example given in [2]

$$(W_\psi)(a,b) := |a|^{-1/2} \int_{-\infty}^{\infty} f(t)\, \overline{\psi(\frac{t-b}{a})}\, dx \qquad (1)$$

for a wavelet $\psi \in L^2(\mathbb{R})$ compared to SAR processing with chirp $\psi \in L^2(\mathbb{R})$

$$(SAR_\psi)(b) := (f * \check{\psi})(b) = \int_{-\infty}^{\infty} f(t)\, \overline{\psi(t-b)}\, dx \quad (2)$$

where $\check{\psi}(t) = \psi(-t)$, i.e. SAR processing is the special case $a = 1$ of wavelet transforming f with no dilations but only translations of ψ. Furthermore, any compactly supported zero-mean chirp ψ fulfills the *admissibility condition* as given in [2] and therefore qualifies as wavelet. This applies to all zero-mean compactly supported waveforms $\psi \in L^2(\mathbb{R})$, [3], therefore, also to chirps. Consequently, any sent chirp in SAR imaging should be zero-mean in order not to falsify acquired SAR raw data in terms of image 'energy'.

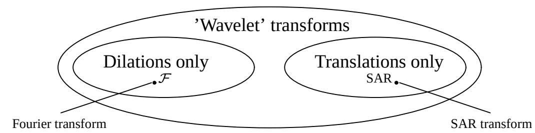

Similarly, and also described in [4], the Fourier transform is an example of the opposite case $b = 0$ of 'wavelet' transforming f where only dilations and no translations of ψ are required for signal construction. But more precisely, we must note that function $\psi(x) = e^{-2\pi i x}$ which is generating the Fourier basis functions $\psi_a(x) = e^{-2\pi i x/a}$ by dilations is strictly *no* wavelet. It does not fulfill the admissibility condition which is part of the wavelet definition. However, the admissibility condition secures two pre-conditions for wavelet transforms. First, it secures that the transform is *isometric*, i.e. no 'energy' is added to the signal during the transformation. This also applies to the Fourier transform [3]. Secondly, it secures that the wavelet is indeed a spatially 'short' wave whose spectrum quickly decays to zero. This is required for allowing the spatial localization of frequencies when analyzing f with wavelet ψ. However, due to the infinite support of Fourier basis functions, frequencies cannot be spatially located which is a considerable disadvantage of the Fourier transform and, actually, led to the invention of wavelet transforms. To consolidate the additional requirement, it was incorporated into the wavelet transform definition. As a conclusion we may say that the Fourier transform is a special case of wavelet transforming with a slightly weaker admissibility condition.

In the following we would like to show that SAR processing is one direction of a data transform, ideally mapping 'lossless' from unfocused to focused SAR images and vice versa. For that, it is first required to review the model of SAR raw data and SAR images. Then we define the discrete SAR transform, prove that it is indeed a transform and compare it to the discrete wavelet transform. Finally, by considering SAR processing as wavelet transform we reason about possibilities to speed up SAR processing. As wavelet transforms may operate in the order of $O(N)$ operations or even $O(log(N))$, they are much faster than employing the Fourier transform with $2 \times O(N\,log(N)) + O(N)$. A very promising technique for fast wavelet transform design is the Lifting Scheme [6].

2 The SAR Raw Data Model

In SAR imaging, we digitally measure radar reflectivity σ as a function $\sigma : \mathbb{R}^2 \rightarrow \mathbb{C}, t \mapsto \sigma(t)$ of its infinite spatially extent on the earth surface $t \in [-\infty, \infty] \times [-\infty, \infty]$. It requires three operations applied to σ for describing the SAR raw data model: windowing, sampling and convolution. Windowing selects the imaged area on ground by multiplication with a rectangle weighting function $rect(t)$ equal to 1 for the imaged area and zero else. Sampling is described in [5] as multiplication with the Dirac series $samp(t) = \sum_{n \in \mathbb{Z}^2} \delta(t - nT)$. And convolution with the backscatter function $\psi(t)$ of a single scatterer on ground is implicitly performed due the SAR imaging geometry. Using sampling rates $T = [T_1, T_2]^\mathsf{T}$, where $T_1 = 1/PRF$, we may write down the

Simplified Raw Data Model:

$$\begin{aligned} raw(t) &= \psi(t) * (samp_{\scriptscriptstyle T}(t) \cdot rect(t) \cdot \sigma(t)) && (3)\\ &= \psi(t) * (\sum_{n \in \mathbb{Z}^2} \delta(t - nT) \cdot \sigma_{rect}(t)) \\ &= \psi(t) * (\sum_{n \in \mathbb{Z}^2} \sigma_{rect}(nT)\, \delta(t - nT)) \\ &= \sum_{n_1=0}^{N_1-1} \sum_{n_2=0}^{N_2-1} \sigma(nT)\, \psi(t - nT) && (4) \end{aligned}$$

which is a simplification because the chirps $\psi(t - nT)$ actually vary with their position $n = [n_1, n_2]^\mathsf{T}$. For describing SAR raw data sufficiently, variations at least in range direction n_2 must be permitted. Thus, we may give the

Standard Raw Data Model:

$$raw_1(t) = \sum_{n_1=0}^{N_1-1} \sum_{n_2=0}^{N_2-1} \sigma(nT)\, \psi_{n_2}(t - nT) \qquad (5)$$

where we have N_2 different two-dimensional chirps for composing the raw image: $\psi_{n_2}(t) \in B = \{\psi_0(t), \ldots, \psi_{N_2-1}(t)\}$, $t \in \mathbb{R}^2$. During $raw_1(t)$ signal construction, the running position parameter n_2 (range position) as part of $n = [n_1, n_2]^\mathsf{T}$ selects a suitable chirp from B. And in general, with also allowing chirp variations with azimuth, we permit individual chirps at each position on ground and call this the

Complete Raw Data Model:

$$raw_2(t) = \sum_{n_1=0}^{N_1-1} \sum_{n_2=0}^{N_2-1} \sigma(nT)\ \psi_{n_1,n_2}(t - nT) \qquad (6)$$

with having $N_1 N_2$ different chirps involved in the raw data construction process $\psi_n(t) \in B = \{\psi_{n_1,n_2}(t) \mid 0 \leq n_l \leq N_l - 1,\ l = 1, 2\}$ such that this model suits for all conceivable SAR applications. The

Ideal Image Model:

$$image(t) = \sum_{n_1=0}^{N_1-1} \sum_{n_2=0}^{N_2-1} \sigma(nT)\ \delta(t - nT) \qquad (7)$$

is derived via (3) by only applying windowing and sampling to σ, omitting convolution.

3 The SAR Transform

When comparing raw data (4),(5),(6) with images (7) then the task of SAR transforming is obviously to switch from $\psi(t)$, $\psi_{n_2}(t)$,$\psi_{n_1,n_2}(t)$, respectively, to $\delta(t)$ and vice versa in all pixel positions n. This can be achieved by inverse convolution, applied in each pixel. For chirps $\psi(t)$ in general, we know that there exists a function $\psi^{-1}(t)$ such that $\psi^{-1}(t) * \psi(t) = \delta(t)$ and, thus, we may define

$$SAR_\psi^{-1}\{\, raw(t)\, \} := \psi^{-1}(t) * raw(t) \qquad (8)$$

which inverts the two-dimensional convolution

$$SAR_\psi\{\, image(t)\, \} := \psi(t) * image(t) \qquad (9)$$

implicitly performed in (3) while SAR raw data acquisition. We call (8) and (9) the SAR transform, SAR^{-1} corresponds to SAR processing. The SAR^{-1} transform on models (5) and (6) is defined as choosing correspondingly ψ_n^{-1} such that $\psi_n^{-1} * \psi_n = \delta$ in each position n.

The *Inverse Filter Approach* employs

$$\psi^{-1}(t) := \mathcal{F}^{-1}\{1/\mathcal{F}\{\psi(t)\}\} \qquad (10)$$

which is the Fourier transform $\mathcal{F}$ of the above equation $\psi^{-1}(t) * \psi(t) = \delta(t)$. However, as real data are always noisy, implementing this approach leads to amplified noise as a result of limited system bandwidth and the chirp spectrum envelope inversion outside the actual bandwidth.

The *Matched Filter Approach* uses

$$\psi^{-1}(t) \approx \overline{\psi(t)}$$

the complex conjugate of $\psi(t)$ as an approximate inverse chirp in (8) for defining the inverse SAR transform. This approach avoids divisions by small numbers as they occur in (10) and is therefore noise-stable. A major drawback is that due to $\overline{\psi(t)} * \psi(t) * image(t) \approx sinc(t) * image(t)$ the resulting image is convolved with an approximate

$sinc(t) := sin(t)/t$ function. This deteriorates the image considerably in terms of resolution and introduces sidelobes. It leads to the

SAR Image Model:

$$\tilde{image}(t) = \sum_{n_1=0}^{N_1-1} \sum_{n_2=0}^{N_2-1} \sigma(nT)\; sinc(t - nT). \tag{11}$$

Consequently, the SAR transform is actually not 'lossless' when applied to noisy data or using the Matched filter. However, the approximation is still good enough if the transform is not iterated several times back and forward but only performed once in inverse direction for SAR processing. The ideal transform model may, nevertheless, help us finding an approach for faster SAR processing methods using wavelet techniques.

3.1 The Discrete 2D SAR Transform

Remembering that $\delta(t - nT)$ is a 'function' whose support is a single pixel at time nT, $image(t)$ may be written in matrix form

$$S = \{\, \sigma(nT)\, \}_n = \{\, \sigma(n_1T_1, n_2T_2)\, \}_{\substack{0 \,\le\, n_1 \,\le\, N_1 - 1 \\ 0 \,\le\, n_2 \,\le\, N_2 - 1}}$$

with $S \in \mathbb{C}^{N_1,N_2}$ only writing down the coefficients of $\delta(t - nT)$ and sum (7) degenerates to a pure construction method. Accordingly, let C, C^{-1}, R be the matrices for discretely representing $\psi(t)$, $\psi^{-1}(t)$ and $raw(t)$, respectively. Let C^{-1} denote the inverse of C with respect to matrix convolution. Then the discrete SAR transform with respect to model (4) is

$$R = SAR\{\, S\,\} := C * S \quad \text{and} \tag{12}$$

$$S = SAR^{-1}\{\, R\,\} := C^{-1} * R \tag{13}$$

following (8) and (9). The convolution between matrices is declared as follows: Let c, s be polynomials depending on variables x, y and $C \in \mathbb{C}^{M_1,M_2}$, $S \in \mathbb{C}^{N_1,N_2}$ are the corresponding polynomial coefficients. Then the product polynomial $c(x,y) \cdot s(x,y) = r(x,y)$ has coefficient matrix $R \in \mathbb{C}^{N_1+M_1-1,N_2+M_2-1}$ and, because r is the product of c and s, it is divisible by c or s without remainder. This is the important fact permitting a 'lossless' inverse operation (13).

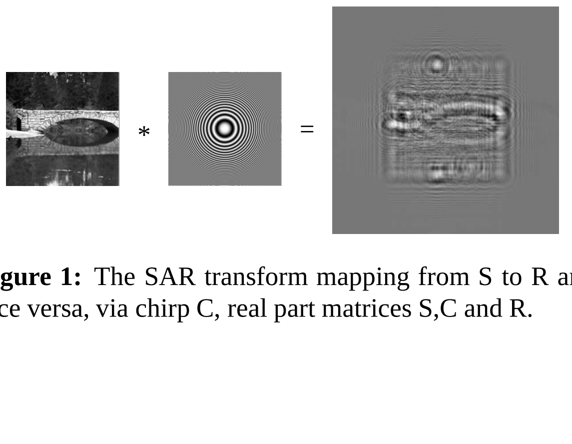

Figure 1: The SAR transform mapping from S to R and vice versa, via chirp C, real part matrices S,C and R.

Furthermore, in Hilbert space $\mathbb{C}^{N_1,N_2}$ with inner product $\langle \cdot, \cdot \rangle$ each matrix $S \in \mathbb{C}^{N_1,N_2}$ is a linear combination

$$S = \sum_{n_1=0}^{N_1-1} \sum_{n_2=0}^{N_2-1} \langle\, S\,, \mathbf{E_{n_1,n_2}} \rangle\, \mathbf{E_{n_1,n_2}}. \tag{14}$$

of $N_1 \times N_2$ basis matrices $\mathbf{E_{n_1,n_2}}$. Let $\mathbf{E_{n_1,n_2}}$ be the matrix with 1 at position n_1, n_2 and zero else. Then (14) is the 'trivial' decomposition of matrix S. Furthermore, it is the matrix notation of (7) and, thus, raw data model (4) can be written as

$$\begin{aligned} R = C * \sum_{n_1=0}^{N_1-1} \sum_{n_2=0}^{N_2-1} \langle\, S\,, \mathbf{E_{n_1,n_2}} \rangle\, \mathbf{E_{n_1,n_2}} \\ = \sum_{n_1=0}^{N_1-1} \sum_{n_2=0}^{N_2-1} \sigma(n_1T_1, n_2T_2)\; \mathbf{C_{n_1,n_2}} \end{aligned} \tag{15}$$

where $\mathbf{C_{n_1,n_2}} = C * \mathbf{E_{n_1,n_2}} \in \mathbb{C}^{N_1+M_1-1,N_2+M_2-1}$ is the matrix with chirp $C \in \mathbb{C}^{M_1,M_2}$ positioned at $n = [n_1, n_2]^{\mathsf{T}}$ and zero else, $M_1 < N_1$, $M_2 < N_2$. Equation (15) illustrates that SAR raw data are superpositioned 'images' of σ-weighted translated two-dimensional chirps. Furthermore, the SAR transform is obviously a coordinate transform switching from focused basis images $\{\mathbf{E_{n_1,n_2}}\}$ to unfocused basis images $\{\mathbf{C_{n_1,n_2}}\}$ and vice versa. In accordance to model (4) we only use one matrix C to generate all $\{\mathbf{C_{n_1,n_2}}\}$. To describe models (5) and (6), we may use N_2 different and $N_1 \times N_2$ different matrices $\mathbf{C_{n_1,n_2}}$, respectively, for generating the SAR raw data basis $\{\mathbf{C_{n_1,n_2}}\}$.

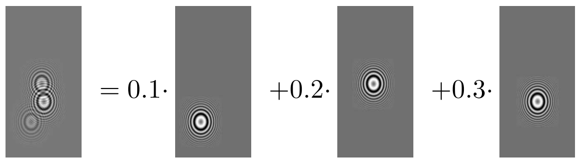

Figure 2: SAR raw data R as superposition of σ-weighted translated chirp matrices $\mathbf{C_{n_1,n_2}}$ with $\sigma = [0.1, 0.2, 0.3]$.

As the two-dimensional chirp $\psi(t) = \psi(t_1, t_2)$ can be written as outer product of two one-dimensional chirps $\psi(t_1, t_2) = \psi_1(t_1) \cdot \psi_2(t_2)$, in matrix notation $C = c_1 c_2^{\mathsf{T}}$ with $c_1 \in \mathbb{C}^{N_1}, c_2 \in \mathbb{C}^{N_2}, C \in \mathbb{C}^{N_1,N_2}$, also the 2D-convolutions in (12) and (13) can be realized as two one-dimensional convolutions such that we may now continue our considerations in the one-dimensional case.

3.2 SAR Transform as Wavelet Transform

According to polynomial multiplication, the convolution of vector $s \in \mathbb{C}^N$ with vector $c \in \mathbb{C}^M$ yields a vector $r \in \mathbb{C}^{N+M-1}$. For simplicity, we also embed vectors s and c in $\mathbb{C}^{N+M-1}$ by filling up zeros and may now use circular convolution $\circledast$ instead $*$ to obtain the same result

$r \in \mathbb{C}^{N+M-1}$. Let $N' = N + M - 1$ and $s_n = \langle s, \mathbf{e_n} \rangle$. In equivalence to (15) we may write

$$r = SAR\{ s \} = \quad c \circledast \sum_{n=0}^{N'-1} \langle s, \mathbf{e_n} \rangle \; \mathbf{e_n} \qquad (16)$$

$$r = \begin{bmatrix} c_0 & 0 & \dots & c_1 \\ c_1 & c_0 & \dots & \vdots \\ \vdots & c_1 & \dots & c_{M-1} \\ c_{M-1} & \vdots & \dots & 0 \\ 0 & c_{M-1} & \vdots & \vdots \\ \vdots & 0 & \dots & 0 \\ 0 & 0 & \dots & c_0 \end{bmatrix} \cdot \begin{bmatrix} s_0 \\ \vdots \\ s_{N'-1} \end{bmatrix} \qquad (17)$$

where matrix $C_{SAR} := c \circledast I \in \mathbb{C}^{N',N'}$ in (17) represents the SAR transform switching from $s \in \mathbb{C}^{N'}$ to $r \in \mathbb{C}^{N'}$. It illustrates, similarly as shown in **Figure 2**, that raw data r are superpositioned s_n-weighted translated chirps c. According to construction, matrix C_{SAR} is invertible and its multiplication inverse C_{SAR}^{-1} must have structure $C_{SAR}^{-1} = (g \circledast I)^{\mathsf{T}}$, i.e. it is composed of translated row vectors g^{T} where $g \in \mathbb{C}^{N'}$ is the convolution inverse of chirp $c \in \mathbb{C}^{N'}$, i.e. $g \circledast c = \mathbf{e_0} = [1, 0, \dots, 0]$.

Hence, we may summarize that on one hand the basis column vectors in C_{SAR} are generated via translations by some waveform c and on the other hand the basis row vectors in C_{SAR}^{-1} are also generated via translations by some waveform g. Chirp c is, according to [2] Definition 3.26, the wavelet spanning the SAR raw data space and g is the corresponding dual wavelet spanning its dual space. The SAR transform is non-orthogonal because c is not self-dual [2]. Theorem 3.27 then confirms the reconstruct ability of SAR images from SAR raw data in the wavelet sense [2].

3.3 The Fast SAR Transform

As derived above, the SAR transform is a wavelet transform not requiring chirp dilations but only translations for constructing or processing SAR raw data. However, for the design of *fast* wavelet transform algorithms the introduction of dilations is computationally required and also practically reasonable. For creating a 'divide and conquer' algorithm following the philosophy of the Fast Fourier Transform (FFT) we may study the Lifting Scheme proposed by Swelden [6]. It allows fast time domain implementations and the construction of Second Generation Wavelets. Applied to SAR processing, the idea is to half the spatially extended chirp size convolved in the data set with each iteration applied. If M is the chirp filter length and N the number of samples then the SAR image should be fully focused after $log(M)$ steps with $O(N)$ operations.

4 Experimental Results

The forward SAR transform based on model (4) is easily been implemented employing polynomial multiplication as described above. For example, product $r(x) = 3x^{10}(1+2x+x^2) = 3x^{10}+6x^{11}+3x^{12}$ realizes a defocusing of coefficient $c_{10} = 3$ at position $n = 10$ with waveform $[1, 2, 1]$. In (5) and (6) we simply vary the convolution kernel, here $[1, 2, 1]$, while summing up. The inverse SAR transform corresponds to re-focusing via polynomial division $s(x) = (3x^{10} + 6x^{11} + 3x^{12})/(1 + 2x + x^2) = 3x^{10}$. Polynomial division is realized via polynomial multiplication but with inverting the chirp using (10). Models (5) and (6) require an inverse convolution kernel update with range or at each pixel, respectively. A 2D-SAR-transform example is depicted in **Figure 1**.

5 Conclusions

In this paper, we modeled SAR processing as transform which is naturally non-orthogonal. We showed that the Inverse Filter on noise-free data corresponds to the ideal transform but Matched filtering is used to control losses in data quality due to noise. We mentioned that the chirp signal which generates SAR raw data is indeed a wavelet and that the SAR transform is a wavelet transform with using chirp translations for signal synthesis (SAR raw data acquisition) and signal analysis (SAR processing). SAR processing as wavelet transform on one hand and the Lifting Scheme as tool for the design of fast wavelet transforms on the other hand might lead to a new type of SAR processing algorithms which is worth to be further investigated.

References

[1] Luc Vignaud: *Radar Imaging, a "Natural" Wavelet Application?* (Invited) in Wavelet and Independent Component Analysis Applications IX, Harold H. Szu, James R. Buss, Editors. Proceedings of SPIE Vol. 4738, pp.264-278, 2002.

[2] Charles K. Chui: *An Introduction to Wavelets* Academic Press, Inc. Harcourt Brace Jovanovich, Publishers, 1992.

[3] Louis/Maaß/Rieder: *Wavelets*, B. G. Teubner Stuttgart, 1994.

[4] Edsward R. Dougherty, Sos S. Againan: *Compression via Orthogonal Transforms, Wavelets, Fractals and Logical Systems*, Short Course Notes, AeroSense 1996, 8-12 April 1996.

[5] Ronald N. Bracewell: *The Fouriertransform And Its Applications*, Second Edition. McGraw-Hill, New York, 1986.

[6] Wim Swelden, Peter Schröder: *Building Your own Wavelets at Home*, SIGGRAPH 96 Course Notes, http://www.multires.caltech.edu/teaching/courses/waveletcourse/athome.pdf.